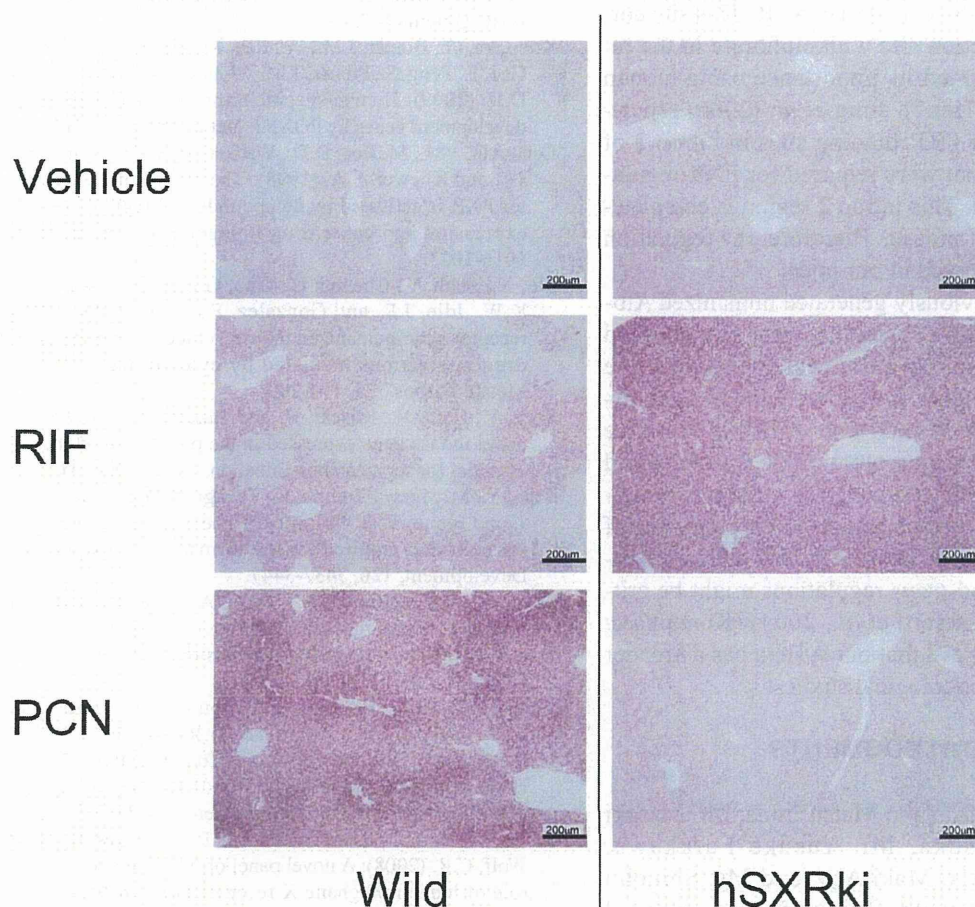


## ISH of Cyp3a11



**Fig. 4.** Humanized response of hSXRki mice to RIF and PCN; *In situ* hybridization for Cyp3a11 mRNA in liver. A DIG-labeled cRNA probe for Cyp3a11 was hybridized and developed for purplish blue chromogenic reaction. Histologically, Cyp3a11 induction was localized around the central veins in both mice with species-specific ligands, respectively.

human-specific ligand RIF to the mice. Induction of the well-known SXR-regulated genes, Cyp3a11 and Ces6 was monitored by Percellome quantitative RT-PCR. As shown in Fig. 3, in the liver and small intestinal mucosa, RIF, but not PCN, induced Cyp3a11 and Ces6 in hSXRki mice (closed column), whereas PCN exclusively induced these genes in WT mice (open column). ISH of Cyp3a11 of the liver also showed humanized responses in hSXRki mice (Fig. 4).

## DISCUSSION

We generated a new humanized mouse model in which the ligand binding domain (LBD) of human SXR was homologously knocked-into the murine SXR gene so that systemic response induced by human-selective SXR ligands can be monitored in mice. Firstly, we showed that mRNA from this chimeric gene was expressed at appropriate levels in the same tissues as the endogenous mouse SXR gene in WT mice. Then the humanized response of the mouse was confirmed by monitoring its response to the human-selective activator RIF, and the lack of response to the rodent-selective activator PCN.

There are relatively few reports about the regulation of SXR expression to date. Aouabdi *et al.* (2006) reported the presence of a PPAR alpha binding site 2.2 kb upstream of the transcription start site in human SXR. This site corresponded to the induction site with clofibrate in the rat and they further confirmed its importance using human liver cancer cell line (Huh7). Jung *et al.* (2006) reported the presence of four FXR binding sites in intron 2 of the mouse SXR gene that were required for FXR regulation of SXR expression. This intron 2 region is completely intact in our hSXRki mouse. Therefore, the regulation by FXR should be preserved in our mice.

Compared to the previously generated humanized Alb-SXR, SXR BAC, and hSXR genome mice, we contend that our hSXRki mouse has an advantage because the human-mouse chimeric gene is expressed in the same tissues and at similar levels to endogenous SXR in WT mice under control of the mouse promoter. This feature would make this model suitable not only for systemic toxicity but also toxicity at various stages of development of the embryo and fetus, maturation of infant, and of senescence, where the *cis* and *trans* regulations might be critical in its regulation (Sarsero *et al.*, 2004) (Konopka *et al.*, 2009). Thus, we believe that our system has a broader application range for toxicological studies.

## ACKNOWLEDGMENTS

The authors thank Ms. Yuko Matsushima, Mr. Masaki Tsuji, Ms. Maki Otsuka, Mr. Yusuke Furukawa, Mr. Kouichi Morita, Ms. Maki Abe, and Ms. Shinobu Watanabe for technical support. This study was supported in part by the Health Sciences Research Grants H19-Toxico-Shitei-001 from the Ministry of Health, Labour and Welfare, Japan.

## REFERENCES

- Aouabdi, S., Gibson, G. and Plant, N. (2006): Transcriptional regulation of the PXR gene: identification and characterization of a functional peroxisome proliferator-activated receptor alpha binding site within the proximal promoter of PXR. *Drug Metab. Dispos.*, **34**, 138-144.
- Bertilsson, G., Heidrich, J., Svensson, K., Asman, M., Jendeberg, L., Sydow-Bäckman, M., Ohlsson, R., Postlind, H., Blomquist, P. and Berkenstam, A. (1998): Identification of a human nuclear receptor defines a new signaling pathway for CYP3A induction. *Proc. Natl. Acad. Sci., USA*, **95**, 12208-12213.
- Blumberg, B., Sabbagh, W.Jr., Juguilon, H., Bolado, J.Jr., van Meter, C.M., Ong, E.S. and Evans, R.M. (1998): SXR, a novel steroid and xenobiotic-sensing nuclear receptor. *Genes. Dev.*, **12**, 3195-3205.
- Jung, D., Mängelsdorf, D.J. and Meyer, U.A. (2006): Pregnane X receptor is a target of farnesoid X receptor. *J. Biol. Chem.*, **281**, 19081-19091.
- Kanno, J., Aisaki, K., Igarashi, K., Nakatsu, N., Ono, A., Kodama, Y. and Nagao, T. (2006): "Per cell" normalization method for mRNA measurement by quantitative PCR and microarrays. *BMC genomics*, **7**, 64.
- Konopka, G., Bomar, J.M., Winden, K., Coppola, G., Jonsson, Z.O., Gao, F., Peng, S., Preuss, T.M., Wohlschlegel, J.A. and Geschwind, D.H. (2009): Human-specific transcriptional regulation of CNS development genes by FOXP2. *Nature*, **462**, 213-217.
- Lehmann, J.M., McKee, D.D., Watson, M.A., Willson, T.M., Moore, J.T. and Kliewer, S.A. (1998): The human orphan nuclear receptor PXR is activated by compounds that regulate CYP3A4 gene expression and cause drug interactions. *J. Clin. Invest.*, **102**, 1016-1023.
- Ma, X., Shah, Y., Cheung, C., Guo, G.L., Feigenbaum, L., Krausz, K.W., Idle, J.R. and Gonzalez, F.J. (2007): The PREgnane X receptor gene-humanized mouse: a model for investigating drug-drug interactions mediated by cytochromes P450 3A. *Drug Metab. Dispos.*, **35**, 194-200.
- Saga, Y., Hata, N., Koseki, H. and Taketo, M.M. (1997): *Mesp2*: a novel mouse gene expressed in the presegmented mesoderm and essential for segmentation initiation. *Genes. Dev.*, **11**, 1827-1839.
- Saga, Y., Miyagawa-Tomita, S., Takagi, A., Kitajima, S., Miyazaki, J. and Inoue, T. (1999): *MesP1* is expressed in the heart precursor cells and required for the formation of a single heart tube. *Development*, **126**, 3437-3447.
- Sakai, K. and Miyazaki, J. (1997): A transgenic mouse line that retains Cre recombinase activity in mature oocytes irrespective of the cre transgene transmission. *Biochem. Biophys. Res. Commun.*, **237**, 318-324.
- Sarsero, J.P., Li, L., Holloway, T.P., Voullaire, L., Gazeas, S., Fowler, K.J., Kirby, D.M., Thorburn, D.R., Galle, A., Cheema, S., Koenig, M., Williamson, R. and Ioannou, P.A. (2004): Human BAC-mediated rescue of the Friedreich ataxia knockout mutation in transgenic mice. *Mamm. Genome.*, **15**, 370-382.
- Scheer, N., Ross, J., Rode, A., Zevnik, B., Niehaves, S., Faust, N. and Wolf, C.R. (2008): A novel panel of mouse models to evaluate the role of human pregnane X receptor and constitutive androstane receptor in drug response. *J. Clin. Invest.*, **118**, 3228-3239.
- Suzuki, T., Akimoto, M., Mandai, M., Takahashi, M. and Yoshimura, N. (2005): A new PCR-based approach for the preparation of RNA probe. *J. Biochem. Biophys. Methods.*, **62**, 251-258.
- Tirona, R.G., Leake, B.F., Podust, L.M. and Kim, R.B. (2004): Identification of amino acids in rat pregnane X receptor that determine species-specific activation. *Mol. Pharmacol.*, **65**, 36-44.
- Watkins, R.E., Wisely, G.B., Moore, L.B., Collins, J.L., Lambert, M.H., Williams, S.P., Willson, T.M., Kliewer, S.A. and Redinbo, M.R. (2001): The human nuclear xenobiotic receptor PXR: structural determinants of directed promiscuity. *Science*, **292**, 2329-2333.
- Xie, W., Barwick, J.L., Downes, M., Blumberg, B., Simon, C.M., Nelson, M.C., Neuschwander-Tetri, B.A., Brunt, E.M., Guzelian, P.S. and Evans, R.M. (2000): Humanized xenobiotic response in mice expressing nuclear receptor SXR. *Nature*, **406**, 435-439.
- Yagi, T., Tokunaga, T., Furuta, Y., Nada, S., Yoshida, M., Tsukada, T., Saga, Y., Takeda, N., Ikawa, Y. and Aizawa, S. (1993): A novel ES cell line, TT2, with high germline-differentiating potency. *Anal. Biochem.*, **214**, 70-76.
- Zhou, C., Tabb, M.M., Sadatrafiei, A., Grün, F. and Blumberg, B. (2004) Tocolinols activate the steroid and xenobiotic receptor, SXR, and selectively regulate expression of its target genes. *Drug Metab. Dispos.*, **32**, 1075-1082.

# Adding Protein Context to the Human Protein-Protein Interaction Network to Reveal Meaningful Interactions

Martin H. Schaefer<sup>1</sup>, Tiago J. S. Lopes<sup>2</sup>, Nancy Mah<sup>1</sup>, Jason E. Shoemaker<sup>2</sup>, Yukiko Matsuoka<sup>2,3</sup>, Jean-Fred Fontaine<sup>1</sup>, Caroline Louis-Jeune<sup>4</sup>, Amie J. Einfeld<sup>5</sup>, Gabriele Neumann<sup>5</sup>, Carol Perez-Iratxeta<sup>4</sup>, Yoshihiro Kawaoka<sup>2,5,6</sup>, Hiroaki Kitano<sup>2,7,8,9</sup>, Miguel A. Andrade-Navarro<sup>1\*</sup>

**1** Computational Biology and Data Mining, Max Delbrück Center for Molecular Medicine, Berlin, Germany, **2** JST ERATO KAWAOKA Infection-induced Host Responses Project, Tokyo, Japan, **3** The Systems Biology Institute, Tokyo, Japan, **4** Sprott Center for Stem Cell Research, Ottawa Hospital Research Institute, Ottawa, Ontario, Canada, **5** Influenza Research Institute, Department of Pathobiological Sciences, School of Veterinary Medicine, University of Wisconsin-Madison, Madison, Wisconsin, United States of America, **6** Institute of Medical Science, Division of Virology, Department of Microbiology and Immunology, University of Tokyo, Tokyo, Japan, **7** Sony Computer Science Laboratories, Inc., Tokyo, Japan, **8** Open Biology Unit, Okinawa Institute of Science and Technology, Okinawa, Japan, **9** Division of Cancer Systems Biology, Cancer Institute, Japanese Foundation for Cancer Research, Tokyo, Japan

## Abstract

Interactions of proteins regulate signaling, catalysis, gene expression and many other cellular functions. Therefore, characterizing the entire human interactome is a key effort in current proteomics research. This challenge is complicated by the dynamic nature of protein-protein interactions (PPIs), which are conditional on the cellular context: both interacting proteins must be expressed in the same cell and localized in the same organelle to meet. Additionally, interactions underlie a delicate control of signaling pathways, e.g. by post-translational modifications of the protein partners - hence, many diseases are caused by the perturbation of these mechanisms. Despite the high degree of cell-state specificity of PPIs, many interactions are measured under artificial conditions (e.g. yeast cells are transfected with human genes in yeast two-hybrid assays) or even if detected in a physiological context, this information is missing from the common PPI databases. To overcome these problems, we developed a method that assigns context information to PPIs inferred from various attributes of the interacting proteins: gene expression, functional and disease annotations, and inferred pathways. We demonstrate that context consistency correlates with the experimental reliability of PPIs, which allows us to generate high-confidence tissue- and function-specific subnetworks. We illustrate how these context-filtered networks are enriched in bona fide pathways and disease proteins to prove the ability of context-filters to highlight meaningful interactions with respect to various biological questions. We use this approach to study the lung-specific pathways used by the influenza virus, pointing to IRAK1, BHLHE40 and TOLLIP as potential regulators of influenza virus pathogenicity, and to study the signalling pathways that play a role in Alzheimer's disease, identifying a pathway involving the altered phosphorylation of the Tau protein. Finally, we provide the annotated human PPI network via a web frontend that allows the construction of context-specific networks in several ways.

**Citation:** Schaefer MH, Lopes TJS, Mah N, Shoemaker JE, Matsuoka Y, et al. (2013) Adding Protein Context to the Human Protein-Protein Interaction Network to Reveal Meaningful Interactions. *PLoS Comput Biol* 9(1): e1002860. doi:10.1371/journal.pcbi.1002860

**Editor:** Andrey Rzhetsky, University of Chicago, United States of America

**Received:** June 28, 2012; **Accepted:** November 9, 2012; **Published:** January 3, 2013

**Copyright:** © 2013 Schaefer et al. This is an open-access article distributed under the terms of the Creative Commons Attribution License, which permits unrestricted use, distribution, and reproduction in any medium, provided the original author and source are credited.

**Funding:** This work was supported by the Japanese Science and Technology Agency (JST, project ERATO Kawaoka), by the German Ministry of Education and Research (BMBF, grant number 01GS08170), by the Helmholtz Alliance in Systems Biology (Germany), and by United States National Institute of Allergy and Infectious Disease Public Health Service research grants. The funders had no role in study design, data collection and analysis, decision to publish, or preparation of the manuscript.

**Competing Interests:** The authors have declared that no competing interests exist.

\* E-mail: miguel.andrade@mdc-berlin.de

## Introduction

The advent of high-throughput techniques to measure and perturb molecular species in a systematic way has enabled researchers to assess the different layers of cellular metabolism under different experimental conditions. Protein-protein interaction (PPI) networks created by a variety of methods including yeast-two-hybrid (Y2H), mass-spectrometry (MS) and computational predictions [1,2] are valuable research resources, and have been used heavily in the last decade. However, a major drawback of these data is that the artificial expression systems used to reconstruct PPI networks do not take into account two of the many factors that are essential to understand the biology of the cell: first, the time-point at which the proteins are expressed (e.g., cell-cycle

or developmental stage) and second, the tissue or intracellular compartment where the proteins are expressed or located (different organs and tissues have very specific protein compositions). Therefore, two proteins may be reported as interaction partners, although they are expressed in different tissues or at different time-points. While high-throughput studies acknowledge these caveats, PPI databases collect these data without mechanisms explicitly directed to discern the biological plausibility of a reported interaction. Therefore, the selection of proteins expressed in a specific cell type or compartment would allow the generation of subnetworks that more realistically represent biological processes in the respective cell types or cellular compartment.

Several attempts have been made to investigate the tissue-specific binding behavior of single proteins and the spatio-temporal

## Author Summary

Protein-protein-interactions (PPIs) participate in virtually all biological processes. However, the PPI map is not static but the pairs of proteins that interact depends on the type of cell, the subcellular localization and modifications of the participating proteins, among many other factors. Therefore, it is important to understand the specific conditions under which a PPI happens. Unfortunately, experimental methods often do not provide this information or, even worse, measure PPIs under artificial conditions not found in biological systems. We developed a method to infer this missing information from properties of the interacting proteins, such as in which cell types the proteins are found, which functions they fulfill and whether they are known to play a role in disease. We show that PPIs for which we can infer conditions under which they happen have a higher experimental reliability. Also, our inference agrees well with known pathways and disease proteins. Since diseases usually affect specific cell types, we study PPI networks of influenza proteins in lung tissues and of Alzheimer's disease proteins in neural tissues. In both cases, we can highlight interesting interactions potentially playing a role in disease progression.

dynamics of PPI networks [3,4,5,6,7,8]. In a recent study evaluating the characteristics of publicly available PPI databases, we demonstrated that the use of subnetworks (which include only interactions of proteins expressed in the same tissue) identifies potential mechanisms or pathways that would remain obscured if the complete PPI database was used [9].

In addition, many proteins have multiple functions, carried out in cooperation with distinct sets of interacting partners. Networks of interacting proteins with coherent function have been termed context networks [10]. Here, we adopt this notion of context and extend it to PPIs or networks of proteins being expressed in the same tissue or cooperatively transmitting signal flow.

There is a lack of studies testing systematically the potential of adding context information to PPI networks in recovering meaningful PPI subsets and, although there are a few approaches that allow to add expression or functional information to PPI data [11,12,13], convenient methods for the creation of such context-specific subnetworks are generally missing.

Here, we introduce an approach to add context to PPI networks using annotations and relations between the interacting partners and demonstrate that context-specific PPI networks are enriched in high-confidence interactions. We use this approach to investigate how the proteins of the human influenza virus interfere with the immune response of the host cell in a tissue-specific manner, finding novel potential regulators of influenza virus pathogenicity, and to study the brain-specific signaling pathways that play a role in Alzheimer's disease, identifying a pathway involving the altered phosphorylation of the  $\tau$  protein. Thereby, we illustrate how the addition of context to PPI networks can guide researchers in the discovery of meaningful interactions and pathways, which would otherwise be obscured by the vast amount of irrelevant (for a specific question) and partly erroneous amount of PPI data.

## Materials and Methods

### Data sources

Our approach to add context-specific information to human PPI data was implemented in the HIPPIE database [14]. HIPPIE is an integrated PPI database that currently contains more than

101,000 interactions of ~13,500 human proteins. HIPPIE is regularly updated by incorporating interaction data from major expert-curated experimental PPI databases (such as BioGRID [15], HPRD [16], IntAct [17] and MINT [18]) in an automated manner using the web service PSICQUIC [19]. All interactions have an associated confidence score based on the sum of cumulative supporting experimental evidence.

Individual proteins were associated with tissues, subcellular locations and biological processes in the following manner. First, proteins were associated with tissues (based on their gene expression profiles retrieved from BioGPS [20] and using the method defined in [9]) or defined as housekeeping (using a list from [21]). Next, associations with biological processes and subcellular locations were determined according to the EBI Gene Ontology (GO) annotation (release from October 28, 2011; reduced to GO slim terms) [22], and to MeSH terms belonging to "Diseases" (class C) or "Tissues" (class A10) that annotate the biomedical references associated to them in MEDLINE (release 2012; gene2pubmed at NCBI ftp site).

### Context association

We associated an interaction with a tissue when both interactors are expressed in the same tissue (e.g. "lung"). Given a term of a functional ontology, we associated an interaction with this function when both interactors are annotated with either the given functional term or with children of it in the hierarchy of the ontology. For example, the GO term "transport" would be associated with an interaction between a protein annotated as involved in "vacuolar transport" and another protein annotated as involved in "nucleocytoplasmic transport". Functional terms considered were either GO terms or MeSH terms. We excluded the rather unspecific top-level terms 'biological process', 'cellular component' and 'cell'. Additionally, we ignored categories that are associated to less than 20 interactions.

### Edge directionality

Our approach includes a method to infer directed PPIs. This inference of interaction (edge) directionality needs sets of proteins predefined as sinks and sources. As default sources and sinks, we connected all proteins annotated with the GO terms 'receptor' and 'sequence-specific DNA binding transcription factor activity', respectively, in the UniprotKB [23]. This is done assuming that signal pathways follow the transmission of information through interacting proteins starting in cell surface receptors that collect external cues and ending in transcription factors as final effectors on gene regulation, following [24]. To infer edge directionality, all pairwise shortest paths between proteins of the source and the sink sets present in the generated output network are calculated. We do not consider edge weights and, hence we are able to determine each shortest path in linear time via a breadth-first search. An edge of the network is considered to be directed if at least one shortest path goes through that edge. The direction of the path (from source to sink) determines the direction of the edge. Edges with conflicting orientations of passing paths are not assigned directionality.

### Pathway enrichment analysis

For the evaluation of the influenza virus host factor network generation we performed pathway enrichment analysis with ConsensusPathDB (run on August 30, 2012; [25]). We used a cut-off of 0.05 on the q-value, which is the false discovery rate (FDR) adjusted equivalent to the p-value. The background control for the tests was the complete list of proteins annotated as expressed in the given tissues (and with PPI information in HIPPIE).

## Definition of up-regulated genes upon influenza infection

We retrieved the preprocessed microarray data described in [26] measuring gene expression changes over multiple time points in a lung adenocarcinoma cell line (Calu-3) infected with influenza A/Netherlands/602/2009 (H1N1). To select steadily up-regulated genes we filtered for probes differentially expressed at the last three time-points in the time series (30, 36 and 48 h) with a q-value less than 0.01 and a log<sub>2</sub> fold change greater than 1.

## Literature mining protocol to obtain PPIs associated to Alzheimer's and protein phosphorylation

To generate a list of PPIs related to Alzheimer's and protein phosphorylation, first, we used the webserver MedlineRanker [27] to retrieve a list of ranked PubMed abstracts (corresponding to manuscripts published within the last 5 years) according to their relevance to the search term "Alzheimer phosphorylation", which relates loosely to the question of interest. Next, we input the top 50 abstracts from MedlineRanker into the webserver PESCADOR [28], which extracts a network of potential PPIs based on a set of PubMed abstracts. In our example, PESCADOR outputs 10 interaction pairs (type 2; co-occurrence of genes or proteins within a sentence containing a biointeraction term), of which only 4 pairs existed in HIPPIE as scored interactions (PSEN1:PSEN2, GSK3B:MAP1, APP:BACE1, PPP2R4:SET). These confirmed PPIs were then used as input for further analysis.

## Results

### Context-specific and directed PPI networks

We inferred context information for all interactions in the human PPI database HIPPIE [14]. This database collects human PPIs for which there is experimental evidence. The amount and quality of the experimental evidence supporting each PPI is evaluated with a confidence score that ranges from 0 to 1. In a first step, we associated all 13,477 proteins in HIPPIE with the following attributes: tissue-expression, GO biological process and cellular compartment, and inferred annotations for the MeSH categories disease and tissue. We then inferred context associations to the PPIs according to the annotations of the interacting proteins and taking into account the hierarchical structure of GO and MeSH terms (see Materials and Methods for details).

By assuming that a large fraction of signaling events transmits information from proteins sensing environmental changes to effector proteins altering the cellular state, we computed shortest paths from membrane-bound receptors to transcription factors (TF) through the network. From the predicted information flow we assigned edge directionality to interactions on these paths (see Materials and Methods for details).

Overall, we were able to associate context to more than 97,000 of the 101,131 interactions of the current version of HIPPIE. Interactions for which we inferred or collected annotations had significantly better experimental evidence (Figure 1A). This suggests that annotated interactions might have higher biological significance than non-annotated ones.

As expected, we observed that more specific context categories were associated to interactions with higher experimental reliability: while the confidence scores of interactions with rather unspecific and ubiquitous terms resemble the overall confidence score distribution, interactions with highly specific terms usually have a higher than average confidence score (Figure 1B-C). For example, the 43,372 interactions associated with the GO category 'cytoplasm' (of depth 1 in the GO hierarchy) have an average confidence score of 0.675 as compared the average of 0.670 over

all interactions. On the other hand, the 159 interactions associated with the (depth 3) GO category 'ribonucleoprotein complex assembly' have an average confidence score of 0.754. We observed a similar tendency for more specific MeSH terms to have a higher experimental reliability.

To demonstrate that our automated context association approach allows identification of relevant interactions, we tested if networks of interactions of our inferred MESH-based disease-annotation are enriched in well-known disease proteins. Therefore, we repeatedly generated disease-context networks around a set of canonical disease proteins. As a canonical disease protein specification, we retrieved the manually curated UniProt Knowledgebase disease protein annotation. For each of the canonical disease proteins, we generated two types of networks: (a) disease networks consisting only of interaction partners of the disease proteins that we had associated with the equivalent MeSH disease term and (b) unfiltered PPI network consisting of all interaction partners of the disease protein from HIPPIE. We did this for all disease proteins where the disease was associated with at least two disease proteins in UniProt and at least two interactions that we had associated with this disease. To quantify the enrichment of disease proteins in these networks we repeatedly calculated the F1 score, the harmonic mean of precision and recall ( $F1 = 2 * \text{precision} * \text{recall} / (\text{precision} + \text{recall})$ ). A one-sided Mann-Whitney-test comparing the distribution of F1 scores between the disease networks and the non-filtered networks indicated that the F1 scores for the disease networks were significantly larger ( $p < 0.05$ ) proving an enrichment of disease proteins in the disease filtered networks (without losing sensitivity by removing disease proteins in the filtering step). The mean precision on the filtered networks was 0.47 and on the unfiltered networks 0.21. The mean recall for the filtered networks was 0.14 and for the unfiltered networks 0.15. This illustrates that in exchange for a small decrease in recall the precision can be more than doubled by applying the MeSH disease filter.

We then investigated the potential of edge directionality inference based on the shortest paths between membrane-bound receptors and TFs through the PPI network to recover known pathways. We retrieved pathway annotations (extracted from WikiPathways download March 29, 2012) and computed the shortest paths through HIPPIE between all pairs of receptors and TFs within the same pathway (excluding only pairs that directly interact or could not be connected by any path). We counted the number of proteins of each pathway found on the shortest paths. We found for 3163 of the 5063 pairs that this approach correctly identified proteins of the selected pathway. The mean precision (the fraction of proteins on the paths that indeed belonged to the correct pathway) over all combinations of receptors with transcription factors was 0.20. The mean recall (the fraction of the pathway that was recovered by considering the paths between one receptor and one transcription factor) was 0.02.

To assess if the agreement between shortest paths and canonical pathways was larger than expected by chance, we generated a background distribution by computing repeatedly the shortest paths between a receptor and a TF from different pathways and computed the overlap between the proteins on the shortest paths to either the TF- or the receptor-containing pathway. We found that the overlap distribution was significantly higher when the receptor and the TF were members of the same pathway ( $p < 0.001$ ; Mann-Whitney-test) proving the potential of shortest paths to recover the signal flow between TFs and receptors when functionally related pairs of receptors and transcription factors are chosen.

We wondered if we could further increase the overlap between the shortest paths and the canonical pathways by filtering the networks for tissue expression. To associate pathways with tissues, we determined for each pathway which tissues were enriched

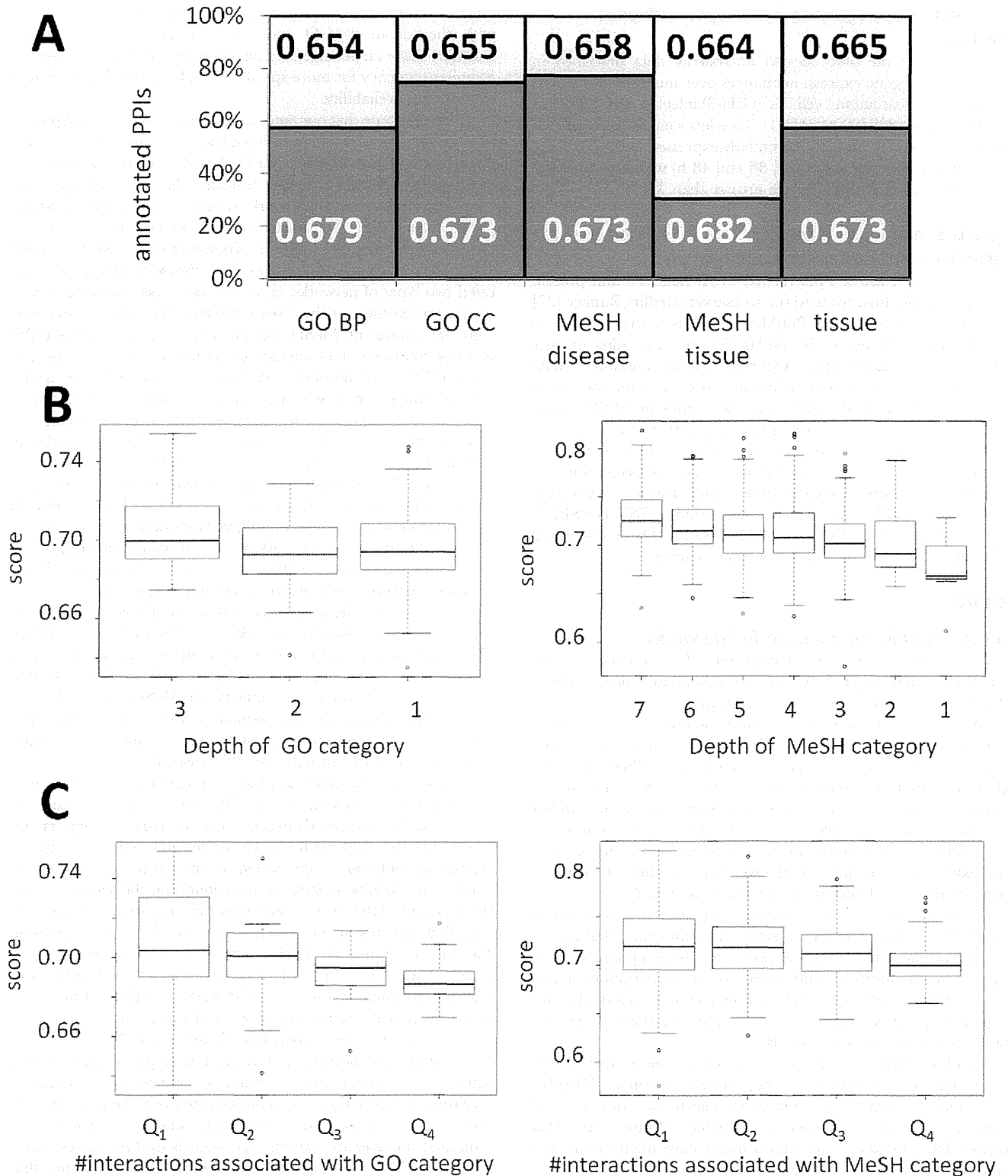


**Figure 1. Experimental reliability of annotated PPIs.** (A) All 101,131 PPIs in HIPPIE are scored according to their associated experimental evidence with a value that ranges from 0 to 1 and increases with the quality and amount of experimental evidence reported in PPI databases [14]. We were able to infer context to a fraction of interactions according to: GO terms biological process (BP) and cellular component (CC), MeSH terms (subcategories disease and tissue) and tissue or housekeeping expression. The numbers in the bars indicate the mean experimental score of the non-annotated fraction (above, black font) and of the annotated fraction (below, white font), respectively. All mean-score differences between annotated and not annotated interactions were significant ( $p < 0.001$ ; Mann-Whitney-test). (B–C) Box plots visualizing the distribution of experimental scores of PPIs associated with GO (left) and MeSH (right) term categories. (B) The scores for GO and MeSH terms decreased generally for less specific terms (the only exception was GO terms depth 2, which was associated with interactions of a lower mean confidence as compared to GO terms depth 1). (C) GO and MeSH terms were subdivided in quartiles according to the number of interactions annotated for each category. The scores decreased for terms associated to higher numbers of interactions. doi:10.1371/journal.pcbi.1002860.g001

among the genes of the pathway (Supplementary Table S1 lists pathway that are associated to more than 2-fold enriched tissues). Inspection of the tissues enriched among proteins forming a pathway revealed that in many cases they indeed reflect plausible locations for pathway activity. For example, immune response pathways were enriched among blood cells and pathways associated with neurodegenerative diseases and addiction in brain-related tissues.

We repeated the computation of shortest paths linking receptors to transcription factors in tissue-specific networks for combinations of pathways and tissues listed in Supplementary Table S1 and for all pairs of receptors and transcription factors that were expressed in the respective tissue. Indeed, we observed an increase of the mean precision to 0.24, which indicates that we could increase the amount of meaningful interactions by additionally filtering for tissue expression. The recall remained low (at 0.03), which is not surprising since many pathway-related proteins were not present in the considered tissue-specific networks and, hence, could not be detected. Again, the amount of pathway proteins on the tissue-specific shortest paths between receptors and TF from the same pathway was significantly larger as compared to shortest paths between receptors and TF from different pathways ( $p < 0.05$ ).

To further investigate if the described context-associations can help to extract pathway information from networks, we compared the frequency of protein pairs being member of the same pathway (as defined by WikiPathways) among tissue-specific PPIs (both proteins were required to be co-expressed in at least one tissue) and compared this frequency to PPIs between proteins that are not expressed in the same tissue. We observed that interacting protein pairs that are expressed in the same tissue are indeed more likely to be in the same pathway as compared to interacting protein pairs that are expressed in disjoint sets of tissues ( $p < 0.001$ ). This, again, demonstrates that the annotations have captured properties related to pathways and suggests that the filtering helps revealing pathway information.

In the next sections we use the context-associated PPI network to obtain novel insights into the mechanisms of human disease: we perform a targeted study of the PPI network surrounding the human proteins that interact with influenza virus proteins to find potential regulators of viral pathogenicity, and we explore the question of whether and how altered protein phosphorylation might be a cause of Alzheimer's disease.

### Context-specific subnetworks of influenza virus host factors identify known disease pathways and suggest novel pathogenesis mechanisms

We analyzed PPI data of human proteins that interact with influenza virus proteins. Influenza viruses infect bronchial epithelial tissue and many cell types in the lung, sometimes resulting in viral pneumonia [29]. We started by obtaining a list of 87 human proteins that have been shown to interact with at least one influenza virus protein in a previous study [30]. From this list, we observed that 23 proteins were expressed in bronchial epithelial tissue (BE1), in whole lung, or in both tissues - we refer to these proteins as first layer host factors. We created the second layer by filtering tissue-specific proteins (expressed in BE1 or whole lung) that interact with members of the first-layer (Figure 2A). Together, the first and second layers compose the tissue-specific PPI subnetworks.

Next, we identified known pathways enriched in the BE1- and lung-specific PPI subnetworks, and found both similarities and differences in the cellular functions of each (see Materials and Methods for details on the enrichment analysis and a full list of enriched pathways in Supplementary Table S2). Both subnetworks showed enrichment for processes related to programmed cell

death and eukaryotic translation. These results are consistent with functions known to be activated or disrupted by influenza virus infection [31,32,33]. In addition, proteins in the BE1 subnetwork exhibited a stronger signature in processes involved with transcriptional regulation, sumoylation, and the regulation of mRNA stability (in particular, the stability of AU-rich element-containing mRNAs). Although these processes tend to be associated with general housekeeping functions, we point out that many cytokine and interferon mRNAs contain AU-rich elements [34]. This observation suggests, hypothetically, that influenza virus proteins may function to dysregulate cytokine mRNA stability in BE1, a function that could impact influenza virus pathogenesis through modulation of immune cell infiltration and function. In relation to sumoylation, it has been noted recently that influenza virus can gain protein functionality during infection by interacting with the sumoylation system of the host cell [35]. On the other hand, the lung subnetwork was uniquely enriched for processes related to cell-substrate adhesion (pathway "signaling events mediated by focal adhesion kinase"). Because cell adhesion is important for maintaining cellular viability and epithelial barrier function, it is possible that influenza virus protein-mediated interference with this process could impact both the amount of virus-inflicted damage upon the lung and dissemination of influenza virus into extra-pulmonary sites.

Cells respond to influenza infection by producing cytokines and chemokines [36,37], while viral proteins counteract this innate immune response. One example of a viral protein that directly interferes on the protein level with cellular immune pathways is NS1 (its involvement in immune response suppression is reviewed in [38]). Here, we noted that the lung PPI subnetwork - which was centered on viral protein-host protein interactions - was enriched for several curated pathways involving Toll-like receptor (TLR) and IL-1 receptor (IL-1R) signaling (e.g., "TLR JNK", "TRAF6 mediated IRF7 activation in TLR7/8 or 9 signalling", "IL-1 JNK", "TLR ECSIT MEKK1 JNK" and "IL1-mediated signaling events"). Although these pathways are expected to be activated in response to viral infection, no previous study has identified any role for any influenza virus protein in perturbing TLR or IL-1R signal transduction. Several host proteins were consistently observed in most/all of the enriched TLR/IL-1R pathways from the influenza PPI lung subnetwork, including IRAK1, TOLLIP and MyD88. Under normal conditions, the IRAK1 kinase associates with TOLLIP (an inhibitory molecule), and upon receptor stimulation, IRAK1 is recruited to the TLR/IL-1R-receptor complex through its interaction with MyD88 (reviewed in [39]). Recruitment results in activation of IRAK1 kinase activity and subsequent activation of MAP kinase pathways, NF- $\kappa$ B-dependent gene expression and interferon  $\alpha$  induction. Altogether, these observations suggest the novel possibility that influenza virus proteins interfere with TLR/IL-1R signaling in lung - possibly by accessing a critical regulator of TLR/IL-1R signal transduction (i.e., IRAK1) - an observation that may have implications for the regulation of pathogenesis associated with influenza virus infections.

A recent study demonstrated that signaling through the IL-1 receptor has a protective effect in mice infected with the pandemic 1918 influenza virus [40]. Another study reported that IL-1 receptor-deficient mice succumbed more easily than wild-type mice to infection with an H5N1 virus of low pathogenicity (A/Hong Kong/486/1997) [41]. Moreover, IL-1 receptor-deficient mice showed reduced inflammatory pathology upon infection with A/Puerto Rico/8/34 (H1N1) influenza virus [42]. Several studies also established that influenza virus infection is sensed by TLR7 in plasmacytoid dendritic cells [43,44,45,46,47,48]. However, none

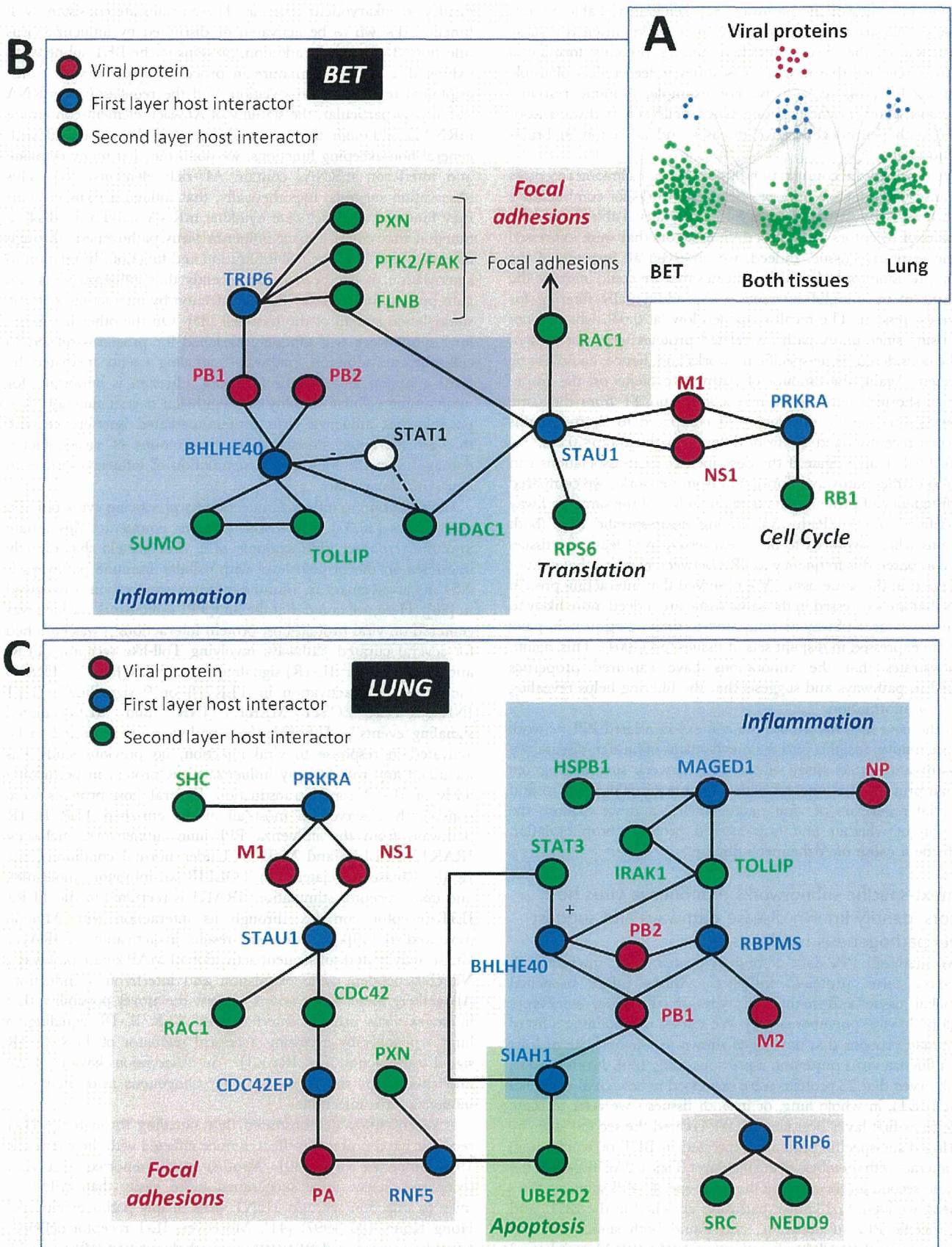


**Figure 2. Tissue-specific PPI subnetwork of human proteins interacting with influenza virus proteins.** (A) Influenza proteins (red) interact with 23 'first layer' host proteins (blue). These first layer proteins have interaction partners that are specific for the bronchial epithelial tissue (BET) subnetwork, for the lung subnetwork or are shared between both subnetworks (all in green). Details of the genes in this figure are given in a



Cytoscape file (File S1). **(B and C)** Mini-networks for BET (B) and lung (C) were created from tissue-specific protein networks linking viral proteins to host proteins whose transcript was up-regulated after influenza virus infection (for a complete list of interactions, see Supplementary Table S4). Viral protein nodes are shown in red, first layer host interactors in blue and second layer host interactors in green. The STAT1 protein (shown in (B) as the white node) was not one of the original network-derived nodes, but was included due to its association with two other network nodes (BHLHE40 and HDAC1) and its known role in mediating inflammation in response to viral infection. General functions associated with different areas in each mini-network (e.g., 'Inflammation' and 'Focal adhesions') are described by partially transparent colored boxes in both (B) and (C). doi:10.1371/journal.pcbi.1002860.g002

of these studies addressed the significance of IRAK1 in influenza virus pathogenicity. Our study thus exemplifies how our network analysis can identify potential regulators of influenza pathogenicity for experimental testing, for example, by assessing influenza virus infections in IRAK1-deficient cells or mice.

Next, we aimed to predict more specific novel interference mechanisms by constructing directed and tissue-specific protein networks linking the viral proteins with proteins whose corresponding transcript was up-regulated after influenza virus infection. We selected steadily up-regulated transcripts from a microarray experiment measuring gene expression changes over time in a lung epithelial cell line infected with a 2009 pandemic H1N1 virus [26] (228 transcripts were selected in total; see Materials and Methods for more details). As expected, all ten most strongly enriched known pathways among the selected transcripts were involved in infection and the immune response. For example, the most highly overrepresented pathway was interferon alpha-beta signaling ( $p < 10e-20$ ).

We constructed BET- and lung-specific networks connecting the viral proteins with the 228 up-regulated factors by shortest paths. From the shortest paths we assigned directions to the edges on these paths. The directed networks consisted of 577 (BET) and 1056 (lung) PPIs. To examine if these networks might reveal relevant information on how viral proteins interfere with the cellular immune response, we tested for enrichment of known pathways in the directed networks. We found that the directed networks were strongly enriched in immune response-related pathways (especially cytokine-related) even after excluding the 228 up-regulated transcripts, indicating that enrichment was independent of the high fraction of immune response factors in the transcriptomics data (Supplementary Table S3). For example, we observed a significant enrichment in both the directed BET- and lung-specific networks for proteins related to IL-2 and IL-6 signaling and focal adhesions ( $q$ -values  $< 0.05$ ). This suggested that we, indeed, might have captured relevant crosstalk between the viral proteins and immune pathways. The full networks are included in the File S1.

To mine the directed networks for interactions that are involved in interference mechanisms of the viral proteins with the cellular immune response, we concentrated, again, on layer one and two host factor proteins on the shortest paths. From the list of curated pathways enriched in both the BET and the lung directed networks (Supplementary Table S3), we selected several cytokine-related pathways (marked in Supplementary Table S3) and filtered for interactions where the second layer protein was in one of these pathways but the layer one protein was not (to specifically detect novel, indirect interference mechanisms). This resulted in a comprehensive BET network consisting of 49 interactions and a lung network formed by 67 interactions including viral proteins and host factors up to layer two (see Supplementary Table S4 for the comprehensive networks and Figure 2 for a manually curated subset of these networks).

Close inspection of these comprehensive cytokine-related networks in both BET and lung revealed several points of potential viral protein-mediated interference with inflammatory pathways (Figure 2). For example, the BET network showed interactions between viral polymerase complex proteins (i.e., PB1 and PB2) and BHLHE40, a transcriptional regulator that cooperates with

HDAC1 to repress STAT1 activity [49] (Figure 2B). STAT1 is essential for the activation of interferon stimulated genes, which repress viral replication, and while influenza virus has an established ability to impair STAT1 [50], no such function has been assigned to any of the viral polymerase complex subunits. BHLHE40 also interacts with TOLLIP, a suppressor of TLR signaling [51] (see also the discussion of lung-specific inflammatory pathways above). This implies that the BHLHE40 protein could act as an important access point for influenza virus-mediated interference with host antiviral and inflammatory regulation in BET, and further that viral polymerase subunits may have an important yet unappreciated role in this activity.

As in BET, lung-specific cytokine-related networks revealed that influenza virus proteins interface with TOLLIP (Figure 2C). However, it is notable that, in lung, this interaction occurs through BHLHE40 and two additional routes (i.e., MAGED1 and RBPMS), potentially involving up to four viral proteins: (i) the aforementioned polymerase complex subunits, PB1 and PB2; (ii) the viral ion channel protein, M2; (iii) and the viral RNA-binding nucleoprotein, NP. Thus, access to TOLLIP might be particularly important in lung. The PB1/PB2-BHLHE40 interaction is maintained in this tissue type, although the nature of the interaction may differ compared to BET. Specifically, BHLHE40 may favor interaction with STAT3 (Figure 2C), and previous evidence indicates that BHLHE40 stimulates STAT3 activity rather than inducing inhibition [52]. Thus, analysis of context-specific PPIs in combination with influenza virus-induced changes in the cellular transcriptome reveal important, putative tissue-specific differences in the ability of viral proteins to interact with cellular immune response signaling networks. Additional experiments will be necessary to further establish the functions of these interactions.

### Search for phosphorylation-dependent PPIs related to Alzheimer's

Assuming no prior expert knowledge on a given topic, we applied a systematic protocol which can, in principle, be used to interrogate the PPI network about the involvement of protein interactions in a complex biological question according to current knowledge. In general, altered states of protein phosphorylation affect the PPI network and can lead to pathogenesis. Our goal in this example was to investigate the possible role of protein phosphorylation in Alzheimer's disease (AD), the most common form of dementia. AD is a degenerative disease manifesting in the brain, and its cause has been hypothesized to be the formation of protein aggregates leading to neuron death, in particular related to the abnormal phosphorylation of the microtubule-associated protein tau [53].

First, we need to input a list of proteins related to the topic. Using a literature mining protocol (see Materials and Methods for details) we generated a list of PPIs related to Alzheimer's and protein phosphorylation: PSEN1:PSEN2, GSK3B:MAP1, APP:BACE1, and PPP2R4:SET. We then studied the network surrounding these interactors (Figure 3).

The initial PPI network contained 727 interactions (Figure 4A). Interactions could be further filtered on the basis of reasonable criteria, namely by tissue filtering for housekeeping and genes

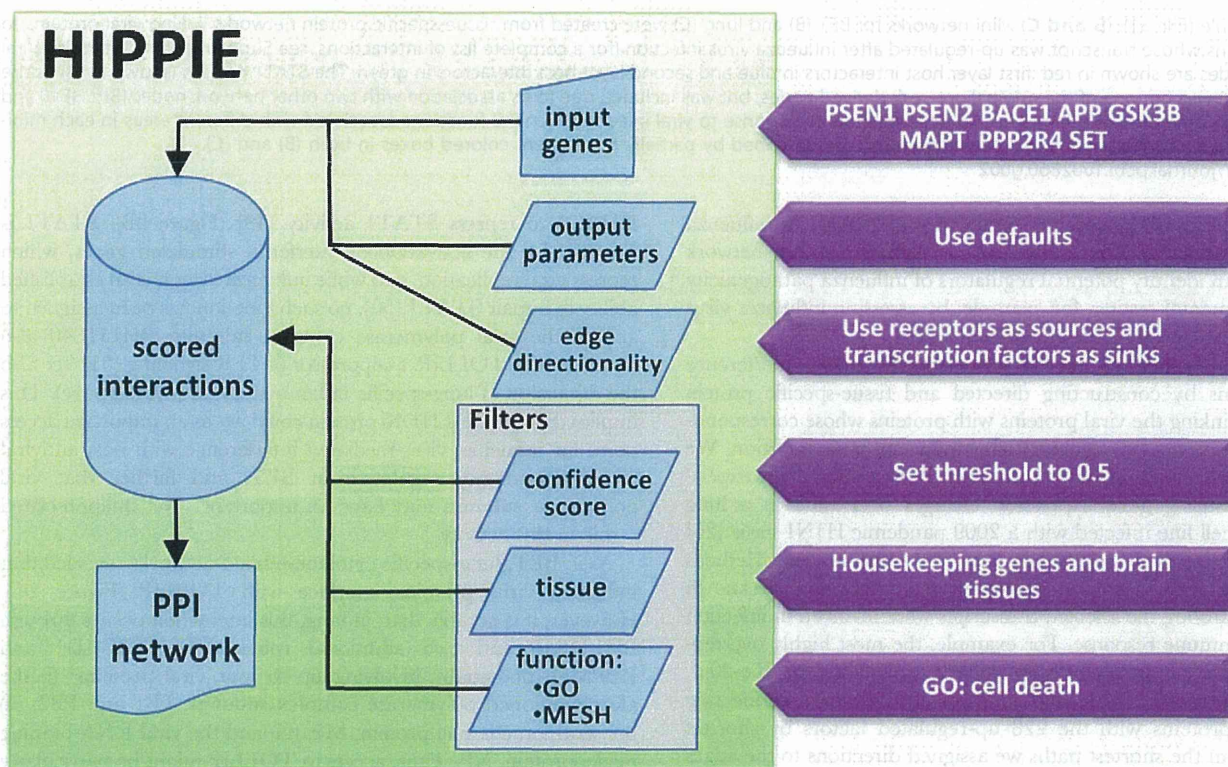


**Figure 3. Protocol for extraction of a PPI subnetwork related to phosphorylation in Alzheimer's disease.** The flowchart illustrates the input terms and options used to generate a topic-focused PPI subnetwork. Eight genes were selected as a result of an unbiased literature mining query for proteins related to Alzheimer's disease (AD) and phosphorylation (see main text for details). The PPI network of first neighbours of these genes in HIPPIE was generated. Then, filters were applied to focus on a PPI subnetwork or proteins expressed in the brain and related to cell death, thus relevant to AD. doi:10.1371/journal.pcbi.1002860.g003

expressed in the brain (we selected “whole brain” and “prefrontal cortex”), and filtering for genes related to the GO term “cell death”, reflecting that AD is characterized by death of neural cells (Figure 4B). Finally, to reveal potential signal transduction pathways we used the inference of edge directionality from receptors to TFs described above (Figure 4B).

Within the resulting network, we highlighted the following path (Figure 4): LRP6-GSK3B-MAP1-AA1F. The low density lipoprotein receptor-related protein 6 (LRP6) interacts with glycogen synthase kinase 3B and attenuates the kinase's ability to phosphorylate microtubule associated protein tau (MAP1) [54]. Tau protein can contribute to AD in different ways: 1) the hyperphosphorylation of tau protein can affect microtubule stability, leading to a disassociation of tau protein from the microtubule, possibly followed by the aggregation of phosphorylated tau into neurofibrillary tangles, which are observed in the brains of AD patients [55]; 2) mediated by protein phosphatase 1 and GSK3 activity, Tau filaments interfere with axonal transport in the neuron, which is consistent with deficiencies in axonal transport in AD [56]. Tau protein has been found to co-localize in the cytoplasm with Che-1 (AA1F), which is an evolutionarily conserved RNA polymerase II binding protein that accumulates in the cell upon DNA damage [57]. It appears that Che-1/Tau proteins dissociate during neuronal cell death [58]; however, the function of Che-1 in the cytoplasm is unclear, as Che-1 is a nuclear protein that is involved in gene regulation of E2F1 targets and p53 and has pro-proliferative and anti-apoptotic functions [59]. Together, these interactions suggest a complex interplay whereby the Tau phosphorylation state and structure, and context-dependent protein distribution within the cell may contribute to

neuronal cell death and AD pathology. An unbiased search for protein phosphorylation in relation to cell death in AD pointed us to this interesting pathway.

## Discussion

The incorporation of tissue-specific expression information to create PPI subnetworks is a useful method to elucidate biological processes that cannot be observed when using the complete PPI network. Here we have shown an approach for the inference of associated context for PPIs based on the annotations of the interacting partners, which enhances the relevance of the annotated interactions. Interactions between proteins expressed in the same location (e.g. lung) or at the same time or developmental stage (e.g. embryo development) can then be selected. Directed pathways can be inferred and highlighted in the filtered network according to sets of sources and sinks corresponding to receptors and transcription factors. Using this approach we were able to identify novel, tissue-specific interactions between influenza virus proteins and cellular inflammatory signaling pathways that may regulate pathogenesis associated with infection, and to describe a brain-specific protein phosphorylation pathway relevant for Alzheimer's disease.

Several methods exist to create subnetworks of the human interactome based on context criteria. For example, POINeT [11] integrates the major PPI databases and allows the creation of tissue-specific networks. To our knowledge we are the first to combine edge directionality, gene expression and functional information for the detection of meaningful interactions. Some approaches exist that infer information flow in a network from the shortest paths (or ‘lowest costs’ if costs are associated with edges)

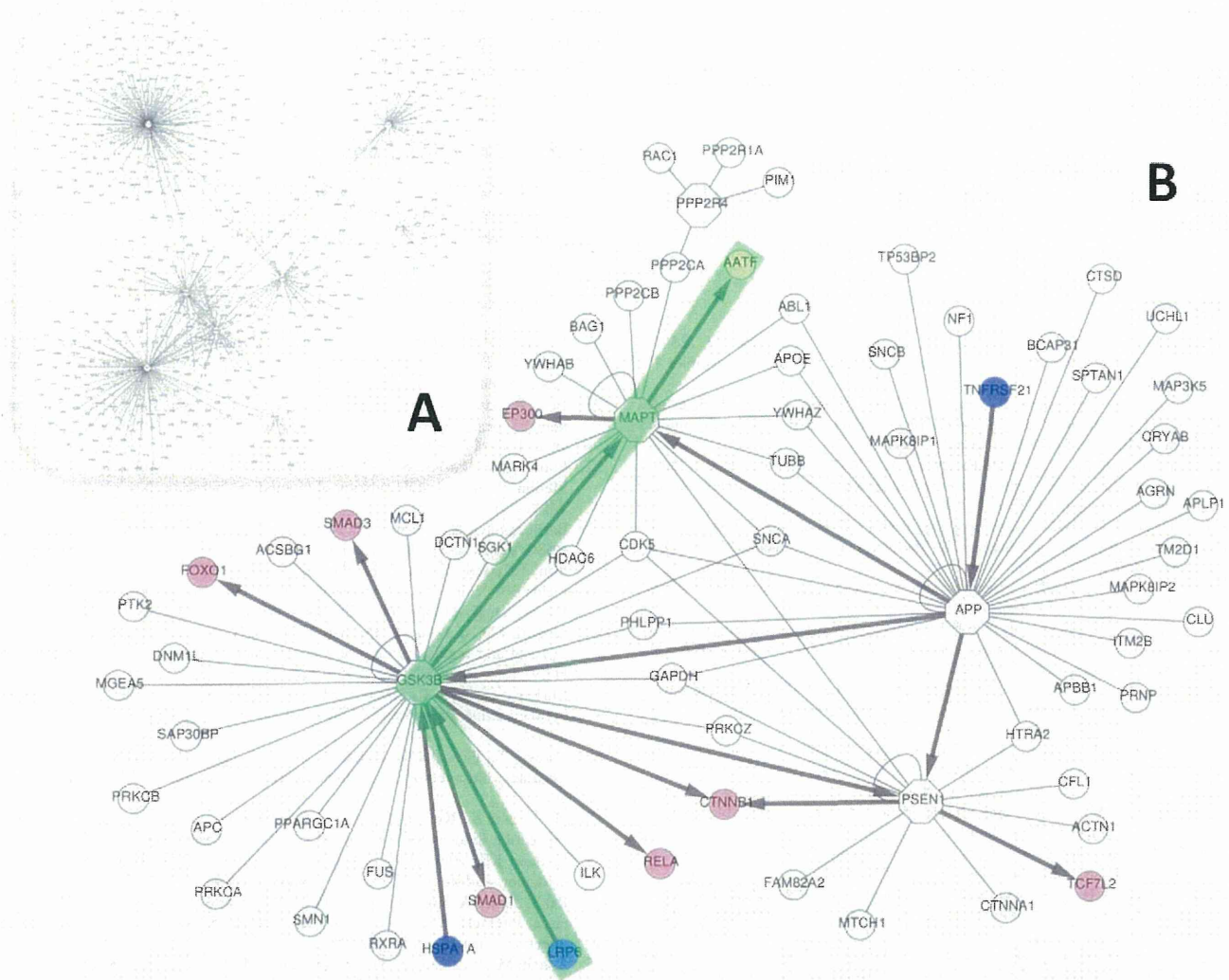


**Figure 4. Filtering and highlighting a PPI subnetwork related to phosphorylation in Alzheimer's disease.** A PPI network was generated as explained in Figure 3 starting with 8 genes relevant for Alzheimer's disease (AD) and phosphorylation. (A) The PPI network contains 727 interactions. (B) Filtering for interactions between partners that are housekeeping or expressed in the brain ("whole brain" and "prefrontal cortex"), relate to the GO term "cell death", and with experimental scores above 0.5, results in a much more focused subnetwork involving 6 of the 8 genes used as input (octagonal nodes). Nodes corresponding to receptors and transcription factors are colored (blue and pink nodes, respectively). Edge directed path analysis from receptors to transcription factors resulted in the association of directionality to some of the edges (arrows). The path LRP6-GSK3B-MAPT-AATF is highlighted in green and described in the text. doi:10.1371/journal.pcbi.1002860.g004

that connects a set of source nodes with sink nodes. Cytoscape plug-ins such as BisoGenet [60] and GenePro [61] find the shortest paths between nodes of the gene and protein network and represent properties of the nodes. SPIKE [62] includes curated pathway data and also calculates pathway inference. The task of identifying signaling events from PPI data and functional protein annotation alone has been addressed in several studies [24,63,64] and implemented in tools (e.g. ANA1 [65]). Here, we proposed a protocol for edge directionality prediction based on calculating the shortest paths between sources and sinks. This protocol is runtime-efficient, which allowed us to provide it as a web tool that is the first to combine both PPI analysis for inference of edge directionality and PPI filtering by tissue and function (available from <http://cbdm.mdc-berlin.de/tools/hippie/>).

In summary, we have presented and made available an approach to associate context to PPI networks, which provides

novel biological insight into mechanisms of disease. The continuing generation of PPI data and further incorporation into databases, and an increasing quality of annotations attached to genes and proteins will result in further improvements of our methodology.

### Supporting Information

**File S1** Network of first and second layer host factors (Figure 2A) in Cytoscape format. (ZIP)

**File S2** Directed BE1 and lung specific networks connecting first layer viral interactors with upregulated host proteins in Cytoscape format. In the directed network, sources and sinks are color encoded (viral are red and upregulated proteins brown). Cytokine-related proteins are shown as circles. (ZIP)

**Table S1** Tissues more than two-fold enriched among proteins in pathways.  
(XLS)

**Table S2** Pathways enriched in first and second layer influenza host factor networks.  
(XLS)

**Table S3** Pathways enriched among directed networks connecting viral proteins with gene products upregulated upon influenza infection.  
(XLS)

## References

- Ramirez F, Schlicker A, Assenov Y, Lengauer T, Albrecht M (2007) Computational analysis of human protein interaction networks. *Proteomics* 7: 2541–2552.
- Mathivanan S, Periaswamy B, Gandhi TK, Kandasamy K, Suresh S, et al. (2006) An evaluation of human protein-protein interaction data in the public domain. *BMC Bioinformatics* 7 Suppl 5: S19.
- Taylor IW, Linding R, Warde-Farley D, Liu Y, Pesquita C, et al. (2009) Dynamic modularity in protein interaction networks predicts breast cancer outcome. *Nat Biotechnol* 27: 199–204.
- Han JD, Bertin N, Hao T, Goldberg DS, Berriz GF, et al. (2004) Evidence for dynamically organized modularity in the yeast protein-protein interaction network. *Nature* 430: 88–93.
- Bossi A, Lehner B (2009) Tissue specificity and the human protein interaction network. *Mol Syst Biol* 5: 260.
- Lin WH, Liu WC, Hwang MJ (2009) Topological and organizational properties of the products of house-keeping and tissue-specific genes in protein-protein interaction networks. *BMC Syst Biol* 3: 32.
- Agarwal S, Deane CM, Porter MA, Jones NS (2010) Revisiting date and party hubs: novel approaches to role assignment in protein interaction networks. *PLoS Comput Biol* 6: e1000817.
- de Lichtenberg U, Jensen LJ, Brunak S, Bork P (2005) Dynamic complex formation during the yeast cell cycle. *Science* 307: 724–727.
- Lopes TJ, Schaefer M, Shoemaker J, Matsuoka Y, Fontaine JF, et al. (2011) Tissue-specific subnetworks and characteristics of publicly available human protein interaction databases. *Bioinformatics* 27: 2414–2421.
- Rachlin J, Cohen DD, Cantor C, Kasif S (2006) Biological context networks: a mosaic view of the interactome. *Mol Syst Biol* 2: 66.
- Lee SA, Chan CH, Chen TC, Yang CY, Huang KC, et al. (2009) POINet: protein interactome with sub-network analysis and hub prioritization. *BMC Bioinformatics* 10: 114.
- Yang L, Walker JR, Hogenesch JB, Thomas RS (2008) NetAtlas: a Cytoscape plugin to examine signaling networks based on tissue gene expression. *In Silico Biol* 8: 47–52.
- Chowdhary R, Tan SL, Zhang J, Karnik S, Bajic VB, et al. (2012) Context-specific protein network miner—an online system for exploring context-specific protein interaction networks from the literature. *PLoS One* 7: e34480.
- Schaefer MH, Fontaine JF, Vinayagam A, Porras P, Wanker EE, et al. (2012) HIPPIE: Integrating Protein Interaction Networks with Experiment Based Quality Scores. *PLoS One* 7: e31826.
- Stark C, Breitkreutz BJ, Chatri-Aryamontri A, Boucher L, Oughtred R, et al. (2011) The BioGRID Interaction Database: 2011 update. *Nucleic Acids Res* 39: D698–704.
- Keshava Prasad TS, Goel R, Kandasamy K, Keerthikumar S, Kumar S, et al. (2009) Human Protein Reference Database—2009 update. *Nucleic Acids Res* 37: D767–772.
- Kerrien S, Aranda B, Breuza L, Bridge A, Broackes-Carter F, et al. (2012) The IntAct molecular interaction database in 2012. *Nucleic Acids Res* 40: D841–846.
- Licata L, Briganti L, Peluso D, Perfetto L, Iannuccelli M, et al. (2012) MINT, the molecular interaction database: 2012 update. *Nucleic Acids Res* 40: D857–861.
- Aranda B, Blankenburg H, Kerrien S, Brinkman FS, Geol A, et al. (2011) PSICQUIC and PSISCORE: accessing and scoring molecular interactions. *Nat Methods* 8: 528–529.
- Wu C, Orozco C, Boyer J, Leglise M, Goodale J, et al. (2009) BioGPS: an extensible and customizable portal for querying and organizing gene annotation resources. *Genome Biol* 10: R130.
- Eisenberg E, Levanon EY (2003) Human housekeeping genes are compact. *Trends Genet* 19: 362–365.
- Dimmer EC, Huntley RP, Alam-Faruque Y, Sawford T, O'Donovan C, et al. (2012) The UniProt-GO Annotation database in 2011. *Nucleic Acids Res* 40: D565–570.
- Magrane M, Consortium U (2011) UniProt Knowledgebase: a hub of integrated protein data. *Database (Oxford)* 2011: bar009.
- Vinayagam A, Stelzl U, Foulle R, Plassmann S, Zenkner M, et al. (2011) A directed protein interaction network for investigating intracellular signal transduction. *Sci Signal* 4: rs8.
- Kamburov A, Pentchev K, Galicka H, Wierling C, Lehrach H, et al. (2011) ConsensusPathDB: toward a more complete picture of cell biology. *Nucleic Acids Research* 39: D712–D717.
- Li C, Bankhead A, 3rd, Eisfeld AJ, Hatta Y, Jeng S, et al. (2011) Host regulatory network response to infection with highly pathogenic H5N1 avian influenza virus. *J Virol* 85: 10955–10967.
- Fontaine JF, Barbosa-Silva A, Schaefer M, Huska MR, Muro EM, et al. (2009) MedlineRanker: flexible ranking of biomedical literature. *Nucleic Acids Res* 37: W141–146.
- Barbosa-Silva A, Fontaine JF, Donnard ER, Stussi F, Ortega JM, et al. (2011) PESCADOR, a web-based tool to assist text-mining of biointeractions extracted from PubMed queries. *BMC Bioinformatics* 12: 435.
- Fields BN, Knipe DM, Howley PM (2007) *Fields virology*. Philadelphia: Wolters Kluwer Health/Lippincott Williams & Wilkins. 2 v. (xix, 3091, 3086 p.) p.
- Shapira SD, Gat-Viks I, Shum BO, Dricot A, de Grace MM, et al. (2009) A physical and regulatory map of host-influenza interactions reveals pathways in H1N1 infection. *Cell* 139: 1255–1267.
- Ehrhardt C, Seyer R, Hrinčius ER, Eierhoff T, Wolff T, et al. (2010) Interplay between influenza A virus and the innate immune signaling. *Microbes Infect* 12: 81–87.
- Ludwig S, Pleschka S, Planz O, Wolff T (2006) Ringing the alarm bells: signalling and apoptosis in influenza virus infected cells. *Cell Microbiol* 8: 375–386.
- He Y, Xu K, Keiner B, Zhou J, Czudai V, et al. (2010) Influenza A virus replication induces cell cycle arrest in G0/G1 phase. *J Virol* 84: 12832–12840.
- Khabar KS (2005) The AU-rich transcriptome: more than interferons and cytokines, and its role in disease. *J Interferon Cytokine Res* 25: 1–10.
- Pal S, Santos A, Rosas JM, Ortiz-Guzman J, Rosas-Acosta G (2011) Influenza A virus interacts extensively with the cellular SUMOylation system during infection. *Virus Res* 158: 12–27.
- Adachi M, Matsukura S, Tokunaga H, Kokubu F (1997) Expression of cytokines on human bronchial epithelial cells induced by influenza virus A. *Int Arch Allergy Immunol* 113: 307–311.
- Matsukura S, Kokubu F, Noda H, Tokunaga H, Adachi M (1996) Expression of IL-6, IL-8, and RANTES on human bronchial epithelial cells, NCI-H292, induced by influenza virus A. *J Allergy Clin Immunol* 98: 1080–1087.
- Hale BG, Randall RE, Ortin J, Jackson D (2008) The multifunctional NS1 protein of influenza A viruses. *J Gen Virol* 89: 2359–2376.
- Gottipati S, Rao NL, Fung-Leung WP (2008) IRAK1: a critical signaling mediator of innate immunity. *Cell Signal* 20: 269–276.
- Belisle SE, Tisoncik JR, Korth MJ, Carter VS, Proll SC, et al. (2010) Genomic profiling of tumor necrosis factor alpha (TNF-alpha) receptor and interleukin-1 receptor knockout mice reveals a link between TNF-alpha signaling and increased severity of 1918 pandemic influenza virus infection. *J Virol* 84: 12576–12588.
- Szretter KJ, Gangappa S, Lu X, Smith C, Shieh WJ, et al. (2007) Role of host cytokine responses in the pathogenesis of avian H5N1 influenza viruses in mice. *J Virol* 81: 2736–2744.
- Schmitz N, Kurrer M, Bachmann MF, Kopf M (2005) Interleukin-1 is responsible for acute lung immunopathology but increases survival of respiratory influenza virus infection. *J Virol* 79: 6441–6448.
- Diebold SS, Kaisho T, Hemmi H, Akira S, Reis e Sousa C (2004) Innate antiviral responses by means of TLR7-mediated recognition of single-stranded RNA. *Science* 303: 1529–1531.
- Geeraedts F, Goutagny N, Hornung V, Severa M, de Haan A, et al. (2008) Superior immunogenicity of inactivated whole virus H5N1 influenza vaccine is primarily controlled by Toll-like receptor signalling. *PLoS Pathog* 4: e1000138.
- Liang QL, Luo J, Zhou K, Dong JX, He HX (2011) Immune-related gene expression in response to H5N1 avian influenza virus infection in chicken and duck embryonic fibroblasts. *Mol Immunol* 48: 924–930.
- Lund JM, Alexopoulou L, Sato A, Karow M, Adams NC, et al. (2004) Recognition of single-stranded RNA viruses by Toll-like receptor 7. *Proc Natl Acad Sci U S A* 101: 5598–5603.
- Miettinen M, Sarenva T, Julkunen I, Matikainen S (2001) IFNs activate toll-like receptor gene expression in viral infections. *Genes Immun* 2: 349–355.

**Table S4** Comprehensive BET and lung PPI networks connecting viral proteins with cytokine-related second layer proteins on shortest paths between viral proteins and gene products upregulated upon influenza infection.  
(XLS)

## Author Contributions

Conceived and designed the experiments: MHS TJS YK HK MAAN. Analyzed the data: MHS TJS NM JES YM JFF CLJ AJE GN CPI. Wrote the paper: MHS TJS NM AJE GN MAAN.

48. Xing Z, Harper R, Anunciacion J, Yang Z, Gao W, et al. (2011) Host immune and apoptotic responses to avian influenza virus H9N2 in human tracheobronchial epithelial cells. *Am J Respir Cell Mol Biol* 44: 24–33.
49. Ivanov SV, Salnikow K, Ivanova AV, Bai L, Lerman MI (2007) Hypoxic repression of STAT1 and its downstream genes by a pVHL/HIF-1 target DEC1/STRA13. *Oncogene* 26: 802–812.
50. Pauli EK, Schmolke M, Wolff T, Viemann D, Roth J, et al. (2008) Influenza A virus inhibits type I IFN signaling via NF-kappaB-dependent induction of SOCS-3 expression. *PLoS Pathog* 4: e1000196.
51. Cario E, Podolsky DK (2005) Intestinal epithelial TOLLerance versus iTOLLerance of commensals. *Mol Immunol* 42: 887–893.
52. Ivanova AV, Ivanov SV, Zhang X, Ivanov VN, Timofeeva OA, et al. (2004) STRA13 interacts with STAT3 and modulates transcription of STAT3-dependent targets. *J Mol Biol* 340: 641–653.
53. Chun W, Johnson GV (2007) The role of tau phosphorylation and cleavage in neuronal cell death. *Front Biosci* 12: 733–756.
54. Mi K, Dolan PJ, Johnson GV (2006) The low density lipoprotein receptor-related protein 6 interacts with glycogen synthase kinase 3 and attenuates activity. *J Biol Chem* 281: 4787–4794.
55. Dolan PJ, Johnson GV (2010) The role of tau kinases in Alzheimer's disease. *Curr Opin Drug Discov Devel* 13: 595–603.
56. LaPointe NE, Morfini G, Pigino G, Gaisina IN, Kozikowski AP, et al. (2009) The amino terminus of tau inhibits kinesin-dependent axonal transport: implications for filament toxicity. *J Neurosci Res* 87: 440–451.
57. Passananti C, Fanciulli M (2007) The anti-apoptotic factor Che-1/AA1F links transcriptional regulation, cell cycle control, and DNA damage response. *Cell Div* 2: 21.
58. Barbato C, Corbi N, Canu N, Fanciulli M, Serafino A, et al. (2003) Rb binding protein Che-1 interacts with Tau in cerebellar granule neurons. Modulation during neuronal apoptosis. *Mol Cell Neurosci* 24: 1038–1050.
59. Bruno T, Desantis A, Bossi G, Di Agostino S, Sorino C, et al. (2010) Che-1 promotes tumor cell survival by sustaining mutant p53 transcription and inhibiting DNA damage response activation. *Cancer Cell* 18: 122–134.
60. Martín A, Ochagavia ME, Rabasa LC, Miranda J, Fernandez-de-Cossio J, et al. (2010) BisoGenet: a new tool for gene network building, visualization and analysis. *BMC Bioinformatics* 11: 91.
61. Vlasblom J, Wu S, Pu S, Superina M, Liu G, et al. (2006) GenePro: a Cytoscape plug-in for advanced visualization and analysis of interaction networks. *Bioinformatics* 22: 2178–2179.
62. Elkon R, Vesterman R, Amit N, Ulitsky I, Zohar I, et al. (2008) SPIKE—a database, visualization and analysis tool of cellular signaling pathways. *BMC Bioinformatics* 9: 110.
63. Yosef N, Ungar L, Zalckvar E, Kimchi A, Kupiec M, et al. (2009) Toward accurate reconstruction of functional protein networks. *Mol Syst Biol* 5: 248.
64. Mah N, Wang Y, Liao MC, Prigione A, Jozefczuk J, et al. (2011) Molecular insights into reprogramming-initiation events mediated by the OSKM gene regulatory network. *PLoS One* 6: e24351.
65. Yosef N, Zalckvar E, Rubinstein AD, Homilius M, Atias N, et al. (2011) ANAT: a tool for constructing and analyzing functional protein networks. *Sci Signal* 4: p11.

This Provisional PDF corresponds to the article as it appeared upon acceptance. Fully formatted PDF and full text (HTML) versions will be made available soon.

## Gene regulatory network analysis supports inflammation as a key neurodegeneration process in prion disease

*BMC Systems Biology* 2012, **6**:132 doi:10.1186/1752-0509-6-132

Isaac Crespo (isaac.crespo@uni.lu)  
Kirsten Roomp (kirsten.rump@uni.lu)  
Wiktor Jurkowski (Wiktor.jurkowski@uni.lu)  
Hiroaki Kitano (kitano@symbio.jst.go.jp)  
Antonio del Sol (antonio.delsol@uni.lu)

**ISSN** 1752-0509

**Article type** Research article

**Submission date** 10 May 2012

**Acceptance date** 17 September 2012

**Publication date** 15 October 2012

**Article URL** <http://www.biomedcentral.com/1752-0509/6/132>

Like all articles in BMC journals, this peer-reviewed article can be downloaded, printed and distributed freely for any purposes (see copyright notice below).

Articles in BMC journals are listed in PubMed and archived at PubMed Central.

For information about publishing your research in BMC journals or any BioMed Central journal, go to

<http://www.biomedcentral.com/info/authors/>

© 2012 Crespo *et al.*

This is an open access article distributed under the terms of the Creative Commons Attribution License (<http://creativecommons.org/licenses/by/2.0>), which permits unrestricted use, distribution, and reproduction in any medium, provided the original work is properly cited.

# Gene regulatory network analysis supports inflammation as a key neurodegeneration process in prion disease

Isaac Crespo<sup>1</sup>  
Email: isaac.crespo@uni.lu

Kirsten Rump<sup>1</sup>  
Email: kirsten.rump@uni.lu

Wiktor Jurkowski<sup>1</sup>  
Email: Wiktor.jurkowski@uni.lu

Hiroaki Kitano<sup>2</sup>  
Email: kitano@symbio.jst.go.jp

Antonio del Sol<sup>1,3,\*</sup>  
Email: antonio.delsol@uni.lu

<sup>1</sup> Luxembourg Center for Systems Biomedicine (LCSB), University of Luxembourg, Luxembourg 1511, Luxembourg

<sup>2</sup> The Systems Biology Institute, Tokyo 108-0071, Japan

<sup>3</sup> Luxembourg Centre for Systems Biomedicine (LCSB), University of Luxembourg, Campus Belval, 7, avenue des Hauts fourneaux, Luxembourg L-4362, Luxembourg

\* Corresponding author. Luxembourg Centre for Systems Biomedicine (LCSB), University of Luxembourg, Campus Belval, 7, avenue des Hauts fourneaux, Luxembourg L-4362, Luxembourg

## Abstract

### Background

The activation of immune cells in the brain is believed to be one of the earliest events in prion disease development, where misfolded PrionSc protein deposits are thought to act as irritants leading to a series of events that culminate in neuronal cell dysfunction and death. The role of these events in prion disease though is still a matter of debate. To elucidate the mechanisms leading from abnormal protein deposition to neuronal injury, we have performed a detailed network analysis of genes differentially expressed in several mouse prion models.

## Results

We found a master regulatory core of genes related to immune response controlling other genes involved in prion protein replication and accumulation, and neuronal cell death. This regulatory core determines the existence of two stable states that are consistent with the transcriptome analysis comparing prion infected versus uninfected mouse brain. An *in silico* perturbation analysis demonstrates that core genes are individually capable of triggering the transition and that the network remains locked once the diseased state is reached.

## Conclusions

We hypothesize that this locking may be the cause of the sustained immune response observed in prion disease. Our analysis supports the hypothesis that sustained brain inflammation is the main pathogenic process leading to neuronal dysfunction and loss, which, in turn, leads to clinical symptoms in prion disease.

## Keywords

Prion disease, Inflammation, Neurodegeneration, Gene regulatory network, Perturbation, Stable states

## Background

Prion proteins are responsible for a class of fatal neurodegenerative diseases, which affect both humans and animals. Prion disease, like other chronic neurodegenerative disease such as Alzheimer's or Parkinson's diseases, belongs to the class of protein misfolding disease that are characterized, pathologically, by abnormal protein deposition and the formation of amyloid plaques [1]. Prion protein exists in major two isoforms: normal, cellular prion protein (Prion<sup>C</sup>) and abnormal, misfolded prion protein (Prion<sup>Sc</sup>). In most forms of prion disease, the misfolded isoform accumulates in extracellular aggregates. Prion disease is transmissible, the primary route of infection being through the ingestion of abnormal prions.

Several hypotheses have been put forward to explain prion disease pathogenesis, such as Prion<sup>C</sup> loss-of-function, Prion<sup>Sc</sup> gain-of-toxic function, endoplasmic reticulum stress, activation of autophagy and/or apoptotic death pathways, and chronic brain inflammation induced by misfolded protein and neuronal injury [2], but none has emerged so far as the main initiator and/or propagator of the disease [3]. We have used a computational network analysis based on known gene expression data to address this complex question. Our analysis shows that it is brain inflammation that plays a key role in prion disease. The main cellular mediators of brain inflammation are microglia, which are responsible for the first active immune response in the brain. These cells are among the earliest responders but their role in prion disease initiation and progression is still debated. We have examined gene expression data from a recent comprehensive transcriptome study on the initiation and progression of prion disease in mouse [4] using a network analysis-based approach and identified a limited number of immune response-related genes as crucial factors in the disease process. These genes appear to be capable of irreversibly locking a large network of differentially expressed genes (DEG) into a disease state, thus uncovering an essential process of the early steps in disease progression.



There is increasing evidence that the brain and immune system are connected: in both normal and pathological conditions neurons are interacting with immune cells and regulating their activity [5]. Chronic immune activation, especially of microglia, is a common feature of chronic neurodegenerative conditions such as Alzheimer's and Parkinson's [6]. For example, there are many similarities between Alzheimer's disease and prion disease: both diseases are characterized by the protein deposition, significant neuronal degeneration and the morphological activation of microglia and astrocytes [7]. In prion disease, neuropathological data shows that microglia are among the earliest responders to neurodegeneration [8,9] and that microglia proliferate in response to disease-causing prion protein deposition [10].

It has been proposed that diseased states correspond to abnormal stable states in the gene expression landscape, or in other words, disease is reflected by long term differential expression patterns [10][11]. The natural robustness of biological networks allows them to maintain the organism in a healthy state despite the influence of a range of external and internal perturbations. The network robustness is a topological property i.e. is a result of specific connectivity between genes in question. However, abnormal network states occasionally occur under the influence of strong internal or external perturbations (i.e. disease initiators or irritants), and these may play an important role in disease initiation and progression. Thus a particular connectivity pattern that is responsible for the robustness of the healthy state can also produce a robust diseased state.

Here we address the question of how a subset of genes forming a master regulatory core in a gene regulatory network is able to determine the stability of this network in a prion disease context. A previous study has shown that gene interactions forming small bi-stable circuits are implicated in the resilience and progression of human cancers, where the healthy and cancer states were considered to be the two stable states [12]. However, how these isolated small bi-stable circuits contribute to the general mechanism of the network stability (and hence cancer development) is still open. We address this issue by significantly extending the idea of bi-stable circuits to a more comprehensive mechanism, the so called master regulatory core, which could explain how the network shifts from the healthy to the diseased stable state. During our analysis we realized that genes belonging to the master regulatory core are highly connected in the network and largely related to immune response, supporting the idea of the central role of a sustained inflammatory process leading to neuronal dysfunction and death in the prion disease progression.

## **Results**

### **The global and core regulatory networks**

Our initial goal was to build a gene regulatory network based on the differentially expressed genes reported by Hwang *et al.* [4]. The functional relationships, based on gene expression, found in the literature resulted in a global network consisting of 106 genes that are differentially expressed during prion infection (all upregulated), connected with 169 functional relations (all activations). (Figure 1A and Additional file 1).

---

**Figure 1 Fragmentation analysis of the global network. The original global unfragmented network (a), the impact on the network connectivity due to the removal of the sixteen genes belonging to the SCC (b), and an example of the removal of sixteen genes randomly selected (c).** In (b) most of the genes become disconnected and the size of the giant component or the biggest connected graph is only 38 genes. In (c) when removing 16 randomly selected genes, the mean of the giant component was 81.02 nodes (standard deviation of 8.29) for 1000 removals. This figure illustrates the relevant role of the SCC as a connectivity element of the network

---

We then carried out stability analysis performed using a boolean dynamical model to compute network stable states. Afterwards, we identified a set of genes able to trigger the transition between attractors and at the same time lead to the network's persistence in the diseased state. Due to the possibility of there being incomplete information about gene-gene interactions even in the parts of the network which are well known, we based our analysis and conclusions on the network stability and the transition between stable states, avoiding a detailed description of transient states (potentially feasible given that experimental data has several time points) that are more sensitive to the lack of information.

Network dynamics are regulated by the structure of the network through the flow of information through feed-forward and feed-back loops. When we looked for network structures with a exchange of information, we found a unique strongly connected component (SCC) consisting of 16 genes. The hallmark of such a structure is that thanks to specific connectivity the information can flow from one gene to any other in the structure following at least one path (see Methods for detailed explanations). This mutual influence between any pair of genes belonging to the SCC makes this structure relevant in terms of information exchange, and therefore potentially determinant for the network's stability. The SCC is mainly regulatory in nature with only 6 incoming functional relations. This SCC constitutes the regulatory core, and its regulatory impact extends up to 74 genes, so the states of these 74 genes depend on the state of the master regulatory core.

In order to analyze the stability of regulatory core genes alone, we carried out a simulation of network dynamics to determine the stable states of this sub-network in isolation using a Boolean dynamical model. Two stable states were found for the regulatory core, one with all nodes "off" and one with all nodes "on". Extending the simulation to cover genes regulated by the regulatory core (i.e. the core network) produced consistent results: again, we found two stable states, one with all nodes "off" and one with all nodes "on".

The perturbation analysis carried out using a continuous dynamical model showed that all regulatory core genes were capable of triggering the transition from the "off" to the "on" stable states in the core network (Figure 2). But no gene was individually capable of inducing the opposite transition, from the "off" to the "on" state. Therefore, when the "on" state was reached, the system staid locked despite external influences. Only simultaneous down regulation of a set of nodes (theoretically possible but unlikely to occur in practice) affecting several circuits in the regulatory core would be able to reverse the "on" state; otherwise, the system is irreversibly activated supporting the idea that the regulatory core constitutes a master regulatory switch that can be activated by external inputs and is able to maintain the activation of a set of nodes that may be relevant for the progression of prion disease.

---

**Figure 2 Perturbation analysis of a gene in the SCC Perturbation of the TLR2 gene (black diamond), and its effect on the other genes of the SCC.** Y-axis: 0 indicates the “off” state, 1 indicates the “on” state. TLR2 is capable of triggering the transition from the “off” (healthy) to the “on” (disease) stable state for all genes in the SCC. The simulations were performed assuming a continuous dynamical system where the initial states are the attractors previously computed in a discrete model (Boolean). The Y-axis represents the “level of activity” in a range between 0 and 1, and X-axis represents “time” in arbitrary units

---

## Network properties

A network is constituted by nodes (i.e. genes) that are inter-connected by edges (i.e. directed functional relations); expression of some genes can either activate or inhibit expression of other genes in the network. Therefore it is important to recognize genes that have more control over the network. We applied two measures: network fragmentation and betweenness centrality to identify genes that play the role of so called communication hubs (mediators of interactions between other, more peripheral genes). Fragmentation is a measure to assess overall network connectivity and may be helpful to determine the impact of a sub-network on global topology. The fragmentation analysis of the global network produced the following results. The mean of the giant component size for 1000 randomized removals of 16 nodes was 81.02 nodes (standard deviation 8.29), while it was only 38.00 nodes in the case of SCC node removal. The difference between these values is 5.18 times the standard deviation of the random removal values. This indicates that the size of the biggest set of connected nodes was reduced dramatically when we removed the nodes of the SCC instead of a random selection of 16 nodes (Figure 1B and C). These results underlined the relevant role of the SCC as a connectivity element of the global network.

The network presented here was scarcely interconnected, which was also reflected in the betweenness centrality analysis. There was a small group of central genes (mostly belonging to SCC) that has a much larger number of peripheral genes in the network connected to them. Six genes could be considered highly central (normalized betweenness > 1): *TGFBI*, *CSF1*, *TLR2*, *CEBPA*, *LGALS3* and *STAT3*. In total, 25 genes were not peripheral (i.e. they mediated at least one gene connection). There was a significant difference when the betweenness centrality of genes participating in the SCC and the genes in the rest of the network were compared. Median betweenness centrality in the SCC and global networks were 123 and 0, respectively; the distributions in the two groups differed significantly (Mann–Whitney Wilcoxon  $W=163$ ,  $n1=16$ ,  $n2=90$ ,  $p\text{-value}=1.406\text{e-}10$ ) supporting the central role of the regulatory core in the global network. It should be noted that the betweenness centrality is more sensitive than other topological features such as degree or clustering coefficient to data incompleteness (missing genes or interactions) because it depends on the global network structure [13,14].

Having the hubs identified, we asked the question whether the strong connectivity occurs between genes involved in common or distinct biological processes. Modules (clusters of genes sharing functional or topological properties) in the network were distinguished by assigning the pathological prion disease processes (derived from gene ontology annotations, described by Hwang *et al.*) to genes constituting the network core. Four modules were considered: disease-causing prion protein (PrP<sup>Sc</sup>) replication and accumulation, immune response, neuronal cell death and other functions (genes which could not be assigned to any of the previous groups). Inter-modular participation is a measure for identifying genes which link different biological processes and this measure was calculated for all module members.

Three groups can be distinguished according to node role (see materials and methods): (1) one connector hub with high inter-modular participation ( $P > 0.60$ ) and significant within-module connectivity ( $z > 2.5$ ) at the same time highly central (normalized centrality  $> 1$ ): *TGFB1*; (2) satellite connectors, (genes with weak connectivity to other nodes of same function but with high ratio of connections to other modules) that share high centrality (normalized centrality  $> 1$ ): *CSF1*, *TLR2*, *LGALS3* and *STAT3*; (3) less high central satellite connectors (positive normalized centrality): *CEBPD*, *STAT1* and *B2M*; (4) other non-central but inter-module participative genes that are regulated by the SCC and are associated with a different functional category than the regulated gene or are regulating genes of other functions: *CASP1*, *CLU*, *TGFBR2*, *P2RX7*, *NFATC1*, *CXCL10*, *CCND1*, *CYBB*, *AIF1* and *GFAP*. As expected most of the selected hubs and connectors are parts of SCC supporting its assumed role as a transition driver.

### Functional analysis

We have categorized the genes of the core network with regard to the four pathological features described by Hwang *et al.* (Figure 3, Table 1). No genes from the pathological feature category synaptic degeneration were found in the core network, but it should be noted that only one of the 333 DEGs in the original mouse study was a member of this category.

**Figure 3 Functional analysis of core network with pathological features** Genes associated with PrP<sup>Sc</sup> replication and accumulation are in green, with nerve cell death in blue, with immune response (including, microglia/astrocyte activation, leukocyte extravasation, general immune response) in pink. Other genes are indicated in grey. SCC genes are indicated as octagons

**Table 1 Summary of the genes and their functional categories**

Biological function	Genes <sup>a</sup>
Prp(Sc replication and accumulation)	A2M, ABCA1, ADAMTS1, APOD, PTGS1, SERPING1
Immune response	
Complement activation: complement system	C3
Complement activation: coagulation & kallikrein system	PDPN, PROS1
Pattern recognition and other receptor	CD14, CD68, <b>ITGB2</b> , FCGR2B, TREM2, <b>TLR2</b>
Microglia/astrocyte activation related	GFAP, <b>PTPN6</b> , <b>STAT1</b> , <b>STAT3</b> , THBS2, TNFRSF1A, VIM
Cytokine, chemokine and growth factor related	<b>CSF1</b> , <b>CSF1R</b> , <b>CXCL10</b> , <b>CX3CR1</b>
Leukocyte extravasation	<b>CYBB</b> , <b>ITGAX</b> , <b>NCF1</b> , <b>TGFB1</b> , <b>TGFBR1</b> , <b>TGFBR2</b>
Other immune response	<b>AIF1</b> , <b>B2M</b> , CD83, CD86, <b>CEBPA</b> , <b>CEBPD</b> , Ctl2a, <b>HLA-E</b> , <b>IFI27</b> , <b>IFIT3</b> , <b>NFATC1</b> , <b>SBNO1</b>
Cell death	<b>CASP1</b> , <b>CCND1</b> , <b>CLU</b> , <b>HSPB1</b> , <b>HSPB8</b> , <b>ID3</b> , <b>MCL1</b> , <b>RBP1</b> , <b>SOCS3</b> , <b>TGM2</b>